

Synthesis, Characterization, and Reactivity of Niobium and Tantalum Complexes Bearing Metal–Nitrogen Bonds. X-ray Molecular Structure of $[\text{Nb}(\text{C}_5\text{H}_4\text{SiMe}_3)\{\text{NH}(\text{CH}_2)_2\text{-}\eta\text{-NH}_2\}\text{Cl}_3]$ and the Novel Tetranuclear Niobium Oxo Derivative $[\{\text{Nb}(\text{C}_5\text{H}_4\text{SiMe}_3)\text{Cl}(\mu_2\text{-O})\}_4(\text{Cl})_2(\mu_3\text{-O})]$

M. Carmen Maestre,[†] Cristina Paniagua,[†] Eberhardt Herdtweck,[‡] Marta E. G. Mosquera,[†] Gerardo Jiménez,^{*,†} and Tomás Cuenca^{*,†}

Departamento de Química Inorgánica, Universidad de Alcalá, Campus Universitario, 28871 Alcalá de Henares, Spain, and Department Chemie, Lehrstuhl für Anorganische Chemie, Technische Universität München, Lichtenbergstrasse 4, D-85747 Garching bei München, Germany

Received March 27, 2007

The reaction of the cyclopentadienyl-silyl-amido titanium compound $[\text{Ti}\{\eta^5\text{-C}_5\text{H}_4\text{SiMe}_2\text{-}\eta\text{-N}(\text{CH}_2)_2\text{-}\eta\text{-NH}_2\}\text{Cl}_2]$ with group 5 metal monocyclopentadienyl complexes $[\text{MCp}^{\text{R}}\text{Cl}_4]$ ($\text{M} = \text{Nb}, \text{Ta}$; $\text{Cp}^{\text{R}} = \text{C}_5\text{H}_4\text{-SiMe}_3$ (Cp'), C_5Me_5 (Cp^*)) afforded the heterobimetallic complexes $[\text{TiCl}_2\{\eta^5\text{-C}_5\text{H}_4\text{SiMe}_2\text{-}\eta\text{-N}(\text{CH}_2)_2\text{-}\kappa\text{-NH}_2\}\text{MCp}^{\text{R}}\text{Cl}_4]$ ($\text{M} = \text{Nb}$, $\text{Cp}^{\text{R}} = \text{Cp}'$, **2a**; $\text{Cp}^{\text{R}} = \text{Cp}^*$, **2b**; $\text{M} = \text{Ta}$, $\text{Cp}^{\text{R}} = \text{Cp}'$, **3a**; $\text{Cp}^{\text{R}} = \text{Cp}^*$, **3b**). Compounds **2** evolve at room temperature to give a three-component mixture, the chlorosilyl-substituted cyclopentadienyl titanium compound $[\text{Ti}(\eta^5\text{-C}_5\text{H}_4\text{SiMe}_2\text{Cl})\text{Cl}_3]$, the corresponding mononuclear amido-amino, $[\text{NbCp}^{\text{R}}\{\text{NH}(\text{CH}_2)_2\text{-}\eta\text{-NH}_2\}\text{Cl}_3]$ ($\text{Cp}^{\text{R}} = \text{Cp}'$, **4a**; $\text{Cp}^{\text{R}} = \text{Cp}^*$, **4b**), and the dinuclear imido niobium complexes $[\{\text{NbCp}^{\text{R}}\text{Cl}_2\}_2(\mu\text{-N}(\text{CH}_2)_2\text{-}\eta\text{-N})]$ ($\text{Cp}^{\text{R}} = \text{Cp}'$, **5a**; $\text{Cp}^{\text{R}} = \text{Cp}^*$, **5b**). In contrast, the analogue tantalum complexes thermally degraded, when $\text{Cp}^{\text{R}} = \text{Cp}'$ at normal temperature, whereas when $\text{Cp}^{\text{R}} = \text{Cp}^*$ at temperatures higher than 50 °C, they gave a unique tantalum complex, the corresponding mononuclear amido-amino derivative $[\text{TaCp}^{\text{R}}\{\text{NH}(\text{CH}_2)_2\text{-}\eta\text{-NH}_2\}\text{Cl}_3]$ ($\text{Cp}^{\text{R}} = \text{Cp}'$, **6a**; $\text{Cp}^{\text{R}} = \text{Cp}^*$, **6b**). Alternatively, these group 5 complexes were prepared by direct reaction of the monocyclopentadienyl derivatives with the corresponding organic diamine, in the appropriate proportion and reaction conditions. Tantalum amino adducts were observed as intermediate species in the course of such reactions, and even the dinuclear derivative $[\{\text{TaCp}^*\text{Cl}_4\}_2(\mu\text{-NH}_2(\text{CH}_2)_2\text{NH}_2)]$ (**8**) could be isolated. Hydrolysis of the dinuclear imido complex **5a** yielded the tricyclic tetranuclear niobium oxo derivative $[\{\text{NbCp}^{\text{R}}\text{Cl}(\mu_2\text{-O})\}_4(\text{Cl})_2(\mu_3\text{-O})]$ (**9**), which displays an asymmetrical structure as a consequence of the triply connected oxygen site. These compounds were characterized by elemental analysis and NMR spectroscopy, and the crystal structures of **4a** and **9** were determined by X-ray diffraction methods.

Introduction

Transition-metal compounds bearing amido and imido ligands acting as a reactive site^{1–6} continue to generate a great deal of interest^{7–9} because of their crucial role in many catalytic and stoichiometric reactions,^{4–9} such as in olefin metathesis,^{10,11}

amido- and imido-based Ziegler–Natta olefin polymerization,^{12–19} and ring-opening metathesis polymerization.^{20–23} In addition, due to their strong π -donating capability and relative inertness,

* Corresponding authors. Tel: 34918854655 and 34918854767. Fax: 34 918854683. E-mail: tomas.cuenca@uah.es; gerardo.jimenez@uah.es.

[†] Universidad de Alcalá.

[‡] Technische Universität München.

(1) Gómez, M.; Gómez-Sal, P.; Jiménez, G.; Martín, A.; Royo, P.; Sánchez-Nieves, J. *Organometallics* **1996**, *15*, 3579–3587.

(2) Royo, P.; Sánchez Nieves, J. *J. Organomet. Chem.* **2000**, *597*, 61–68.

(3) Anderson, L. L.; Schmidt, J. A. R.; Arnold, J.; Bergman, R. G. *Organometallics* **2006**, *25*, 3394–3406.

(4) Hazari, N.; Mountford, P. *Acc. Chem. Res.* **2005**, *38*, 839–849.

(5) Hanna, T. A. *Coord. Chem. Rev.* **2004**, *248*, 429–440.

(6) Leung, W. H. *Eur. J. Inorg. Chem.* **2003**, 583–593.

(7) Chisholm, M. H.; Rothwell, A. P. In *Amido and Imido Metal Complexes*; Wilkinson, G. G. R. D., McCleverty, J. A., Eds.; Elsevier: Oxford, 1987.

(8) Nugent, W. A.; Mayer, J. M. *Metal–Ligand Multiple Bonds*; Wiley: New York, 1988.

(9) Wigley, D. E. *Organoimido Complexes of the Transition-Metals*; John Wiley and Sons: New York, 1994; Vol. 42, pp 239–482

(10) Ivin, K. I. *Olefin Metathesis*; Academic Press: London, 1983.

(11) Schrock, R. R.; Hoveyda, A. H. *Angew. Chem., Int. Ed.* **2003**, *42*, 4592–4633.

(12) Scollard, J. D.; McConville, D. H. *J. Am. Chem. Soc.* **1996**, *118*, 10008–10009.

(13) Coles, M. P.; Dalby, C. I.; Gibson, V. C.; Clegg, W.; Elsegood, M. R. *J. Chem. Soc., Chem. Commun.* **1995**, 1709–1711.

(14) Antonelli, D. M.; Leins, A.; Stryker, J. M. *Organometallics* **1997**, *16*, 2500–2502.

(15) Coles, M. P.; Dalby, C. I.; Gibson, V. C.; Little, I. R.; Marshall, E. L.; daCosta, M. H. R.; Mastroianni, S. *J. Organomet. Chem.* **1999**, *591*, 78–87.

(16) Feng, S. G.; Roof, G. R.; Chen, E. Y. X. *Organometallics* **2002**, *21*, 832–839.

(17) Gibson, V. C.; Spitzmesser, S. K. *Chem. Rev.* **2003**, *103*, 283–315.

(18) Said, M.; Hughes, D. L.; Bochmann, M. *Dalton Trans.* **2004**, 359–360.

(19) Bolton, P. D.; Mountford, P. *Adv. Synth. Catal.* **2005**, *347*, 355–366.

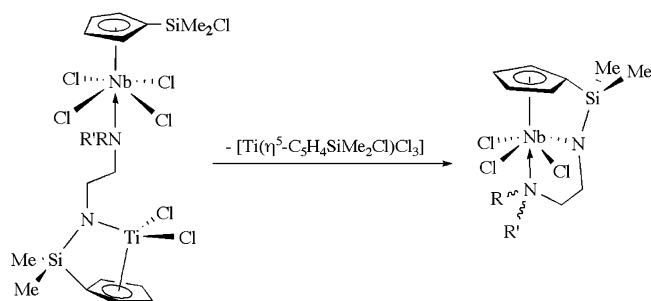
(20) Schrock, R. R. In *Ring Opening Polymerization*; Brunelle, D. J., Ed.; C. Hanser Verlag: Munich, 1993.

(21) Schrock, R. R. *J. Mol. Catal. A: Chem.* **2004**, *213*, 21–30.

(22) Bonanno, J. B.; Veige, A. S.; Wolczanski, P. T.; Lobkovsky, E. B. *Inorg. Chim. Acta* **2003**, *345*, 173–184.

(23) Schrock, R. R. *Acc. Chem. Res.* **1990**, *23*, 158–165.

Scheme 1



these groups have been widely used as convenient ancillary or supporting ligands to stabilize high-oxidation-state early-transition-metal complexes.^{7–9} Consequently, recent decades have witnessed significant progress in the organometallic chemistry of half-sandwich imido complexes of group 5 metals,^{24–33} which has largely been stimulated by the isolectronic relationship^{34,35} between these complexes and the very well known group 4 bent metallocenes extensively used as Ziegler–Natta catalysts.^{36–41} Among the various methods developed for the synthesis of compounds of this kind, simple and efficient routes are the reactions of metal halides with lithium amides or organic amines.^{2,25,30}

We have recently explored the reaction of cyclopentadienyl-silyl-amido titanium derivatives $[\text{Ti}\{\eta^5\text{-C}_5\text{H}_4\text{SiMe}_2\text{-}\eta\text{-N}(\text{CH}_2)_2\text{-NRR}'\}\text{Cl}_2]$ ^{42,43} with the chlorosilyl-substituted cyclopentadienyl niobium compound $[\text{Nb}(\eta^5\text{-C}_5\text{H}_4\text{SiMe}_2\text{Cl})\text{Cl}_4]$,³⁰ which proceeds by the direct transfer of the formal imido ligand $[\text{N}(\text{CH}_2)_2\text{NRR}']^{2-}$ from titanium to niobium (Scheme 1), affording the first example

(24) Blake, A. J.; Collier, P. E.; Dunn, S. C.; Li, W. S.; Mountford, P.; Shishkin, O. V. *J. Chem. Soc., Dalton Trans.* **1997**, 1549–1558.

(25) Herrmann, W. A.; Baratta, W. *J. Organomet. Chem.* **1996**, 506, 357–361.

(26) Humphries, M. J.; Douthwaite, R. E.; Green, M. L. H. *J. Chem. Soc., Dalton Trans.* **2000**, 2952–2959.

(27) Humphries, M. J.; Green, M. L. H.; Douthwaite, R. E.; Rees, L. H. *J. Chem. Soc., Dalton Trans.* **2000**, 4555–4562.

(28) Dubberley, S. R.; Evans, S.; Boyd, C. L.; Mountford, P. *Dalton Trans.* **2005**, 1448–1458.

(29) Galakhov, M. V.; Gómez, M.; Jiménez, G.; Pellinghelli, M. A.; Royo, P.; Tiripicchio, A. *Organometallics* **1994**, 13, 1564–1566.

(30) Alcalde, M. I.; Gómez-Sal, P.; Martín, A.; Royo, P. *Organometallics* **1998**, 17, 1144–1150.

(31) Alcalde, M. I.; Gómez-Sal, M. P.; Royo, P. *Organometallics* **1999**, 18, 546–554.

(32) Arteaga-Müller, R.; Sánchez-Nieves, J.; Royo, P.; Mosquera, M. E. G. *Polyhedron* **2005**, 24, 1274–1279.

(33) Kilgore, U. J.; Yang, X.; Tomaszewski, J.; Huffman, J. C.; Mindiola, D. J. *Inorg. Chem.* **2006**, 45, 10712–10721.

(34) Williams, D. N.; Mitchell, J. P.; Poole, A. D.; Siemeling, U.; Clegg, W.; Hockless, D. C. R.; Oneil, P. A.; Gibson, V. C. *J. Chem. Soc., Dalton Trans.* **1992**, 739–751.

(35) Cockcroft, J. K.; Gibson, V. C.; Howard, J. A. K.; Poole, A. D.; Siemeling, U.; Wilson, C. *J. Chem. Soc., Chem. Commun.* **1992**, 1668–1670.

(36) Jordan, R. F. *Adv. Organomet. Chem.* **1991**, 32, 325–387.

(37) Marks, T. J. *Acc. Chem. Res.* **1992**, 25, 57–65.

(38) Brintzinger, H. H.; Fischer, D.; Mühlhaupt, R.; Rieger, B.; Waymouth, R. M. *Angew. Chem., Int. Ed. Engl.* **1995**, 34, 1143–1170.

(39) Bochmann, M. *J. Chem. Soc., Dalton Trans.* **1996**, 255–270.

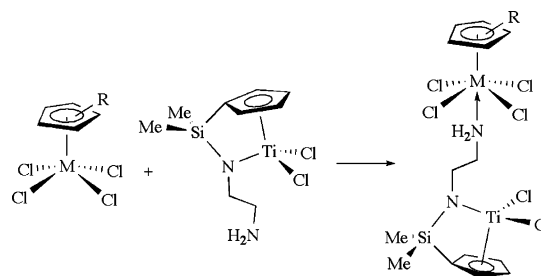
(40) Hlatky, G. G. *Coord. Chem. Rev.* **1999**, 181, 243–296.

(41) Resconi, L. In *Comprehensive Organometallic Chemistry III*; Mingos, M. P., Crabtree, R. H., Eds.; Bochmann, M.; Vol. 4 Ed.; Elsevier: London, 2006; Chapter 9.

(42) Jiménez, G.; Rodríguez, E.; Gómez-Sal, P.; Royo, P.; Cuenca, T.; Galakhov, M. *Organometallics* **2001**, 20, 2459–2467.

(43) Jiménez, G.; Royo, P.; Cuenca, T.; Herdtweck, E. *Organometallics* **2002**, 21, 2189–2195.

Scheme 2



M = Nb, Cp^R = Cp', **2a**; Cp^R = Cp*, **2b**
M = Ta, Cp^R = Cp', **3a**; Cp^R = Cp*, **3b**

of a stable constrained-geometry niobium complex, $[\text{Nb}\{\eta^5\text{-C}_5\text{H}_4\text{SiMe}_2\text{-}\eta\text{-N}(\text{CH}_2)_2\text{NRR}'\}\text{Cl}_3]$.⁴⁴

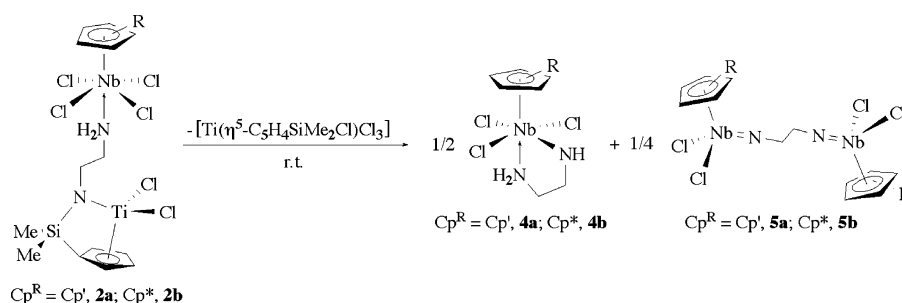
In view of such results, we were interested in probing whether the imido functionality may be similarly transferred to group 5 metals to form terminal imido derivatives, when there is no chlorosilyl substituent on the cyclopentadienyl ring. Thus, we investigated the reaction between $[\text{Ti}\{\eta^5\text{-C}_5\text{H}_4\text{SiMe}_2\text{-}\eta\text{-N}(\text{CH}_2)_2\text{-}\eta\text{-NH}_2\}\text{Cl}_2]$ and different cyclopentadienyl group 5 metal compounds. To achieve such a goal, niobium and tantalum compounds that contain either the trimethylsilylcyclopentadienyl (Cp') or the pentamethylcyclopentadienyl (Cp*) ligand were chosen as starting materials, allowing a suitable and straightforward synthetic route to generate new mononuclear or dinuclear amido, imido, and amino derivatives of group 5 metals. Formation of the heterodinuclear $[\text{TiCl}_2\{\eta^5\text{-C}_5\text{H}_4\text{SiMe}_2\text{-}\eta\text{-N}(\text{CH}_2)_2\text{-}\kappa\text{-NH}_2\}\text{MCp}^R\text{Cl}_4]$ is spectroscopically detected, and syntheses of the amido complexes with a pendant amino group $[\text{MCp}^R\{\text{NH}(\text{CH}_2)_2\text{-}\eta\text{-NHR}\}\text{Cl}_3]$ (M = Nb, Ta; Cp^R = Cp', Cp*; R = H, Me), the tethered dinuclear imido niobium derivatives $[\{\text{NbCp}^R\text{Cl}_2\}_2(\mu\text{-N}(\text{CH}_2)_2\text{-}\eta\text{-N})]$, the amino tantalum complex $[\{\text{TaCp}^*\text{Cl}_4\}_2(\mu\text{-NH}_2(\text{CH}_2)_2\text{NH}_2)]$, and the tetranuclear niobium-oxo compound $[\{\text{NbCp}'\text{Cl}(\mu_2\text{-O})\}_4(\text{Cl})_2(\mu_3\text{-O})]$ are reported in this paper.

Results and Discussion

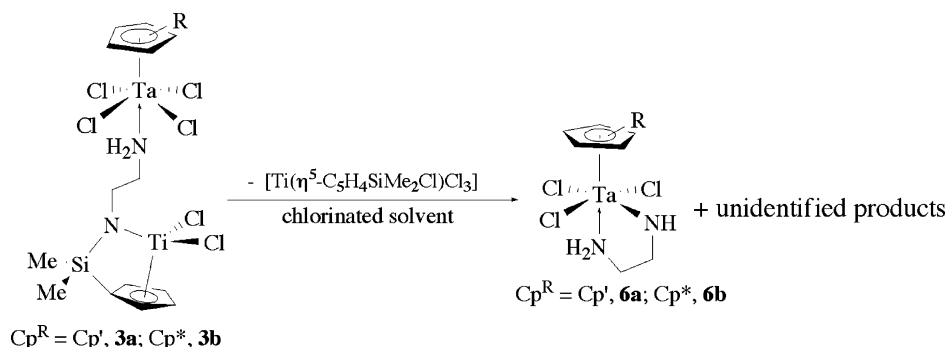
Synthesis and Chemical Behavior of Heterodinuclear Complexes. Reactions of monocyclopentadienyl group 5 metal compounds $[\text{MCp}^R\text{Cl}_4]$ (M = Nb, Ta; Cp^R = C₅H₄SiMe₃ (Cp'), C₅Me₅ (Cp*)) with the cyclopentadienyl-silyl-amido titanium complex $[\text{Ti}\{\eta^5\text{-C}_5\text{H}_4\text{SiMe}_2\text{-}\eta\text{-N}(\text{CH}_2)_2\text{-}\eta\text{-NH}_2\}\text{Cl}_2]$ (**1**) were conducted in Teflon-valved NMR tubes in deuterated solvents, which allowed straightforward spectroscopic characterization of the heterodinuclear complexes $[\text{TiCl}_2\{\eta^5\text{-C}_5\text{H}_4\text{SiMe}_2\text{-}\eta\text{-N}(\text{CH}_2)_2\text{-}\kappa\text{-NH}_2\}\text{MCp}^R\text{Cl}_4]$ (M = Nb, Cp^R = Cp', **2a**; Cp*, **2b**; M = Ta, Cp^R = Cp', **3a**; Cp*, **3b**) (Scheme 2), consistent with their heterodinuclear nature. The ¹H NMR spectra show two sets of signals for the cyclopentadienyl rings (Cp^R and "C₅H₄-Si") along with an AA'BB'KK' spin system for the methylene and amino protons. The signals for the amino protons appear downfield shifted (more pronounced for niobium compounds **2** than for the tantalum derivatives **3**) with respect to the resonances found in complex **1** (δ 4.30),⁴³ indicating that the NH₂ group is fairly strongly coordinated to the group 5 metal. In addition, the significant upfield shift observed in the ¹³C-¹H NMR spectra for the carbon atom *ipso*-C₅H₄SiMe₂N (δ

(44) Maestre, M. C.; Tabernero, V.; Mosquera, M. E. G.; Jiménez, G.; Cuenca, T. *Organometallics* **2005**, 24, 5853–5857.

Scheme 3



Scheme 4



≈ 109) confirms that the titanium atom retains its initial constrained disposition.^{31,44–47}

As previously reported for analogous counterparts Ti–Nb,⁴⁴ these dinuclear species are quantitatively formed (as observed by NMR spectroscopy), although a lack of thermal stability in solution prevented their isolation, as they evolved to a range of products in a short period of time. Prolonged standing of **2** in CDCl₃ or C₆D₆ at room temperature resulted in the formation of a three-component mixture. Along with the titanium compound [Ti(η⁵-C₅H₄SiMe₂Cl)Cl₃], the presence of two niobium derivatives is observed, the mononuclear amido-amino compounds [NbCp^R{NH(CH₂)₂-η-NH₂}Cl₃] (Cp^R = Cp', **4a**; Cp*, **4b**) and the dinuclear complexes [{NbCp^RCl₂}₂(μ-N(CH₂)₂-η-N)] (Cp^R = Cp', **5a**; Cp*, **5b**), which contain two tethered imido functionalities. A ratio of 1(Ti-compound):0.5(amido-amino):0.25(diimido) is obtained (Scheme 3).

These results reveal that the evolution reaction pattern for the heterodinuclear Ti–Nb complexes depends markedly on the nature of the substituent on the cyclopentadienyl ring bonded to the niobium atom. When the niobium derivative with a “SiMe₂Cl” substituent on the Cp ring is studied, a direct transfer of the “H₂N(CH₂)₂N” unit from titanium to niobium regioselectively yields the constrained geometry complex [Nb{η⁵-C₅H₄-SiMe₂-η-N(CH₂)₂NH₂}Cl₃] as the unique niobium product.⁴⁴ In contrast, the absence of a Si–Cl bond on the cyclopentadienyl ligand determines that the reaction should evolve through an aminolysis process of Nb–Cl bonds with the consequent liberation of HCl. The formation of the two different niobium complexes (**4** and **5**) from the heterobimetallic compounds **2** entails a proton-scrambling process. Generation of the amido-amino- and bis-imido-bridged compounds proceeds respectively by gaining one proton and the losing the protons contained in the initial moiety “H₂N(CH₂)₂N”.

The tantalum complexes are comparatively more stable with respect to aminolysis reactions than the analogous niobium derivatives, consistent with the lower Lewis acidity of tantalum. Hence, while the evolution of **3a** is observed in solution at room temperature, the similar complex **3b** remains unperturbed over a prolonged period of time and is only transformed upon heating at temperatures above 50 °C. However, despite repeated attempts to isolate **3b** as an analytically pure substance, intractable mixtures were always obtained. The different stability observed in complex **3b**, compared to **3a**, can be ascribed to the higher electron donor power of the pentamethylcyclopentadienyl ligand.

In chlorinated solvents, compound **3** affords a mixture of compounds, from which two complexes are unambiguously identified. Along with unidentified products the presence of [Ti(η⁵-C₅H₄SiMe₂Cl)Cl₃] and the corresponding mononuclear amido-amino [TaCp^R{NH(CH₂)₂-η-NH₂}Cl₃] (Cp^R = Cp', **6a**; Cp*, **6b**) (Scheme 4) is observed.

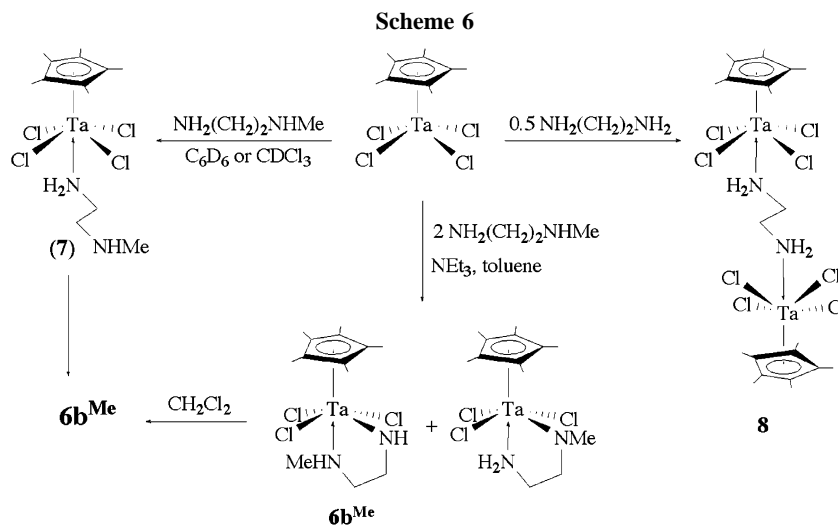
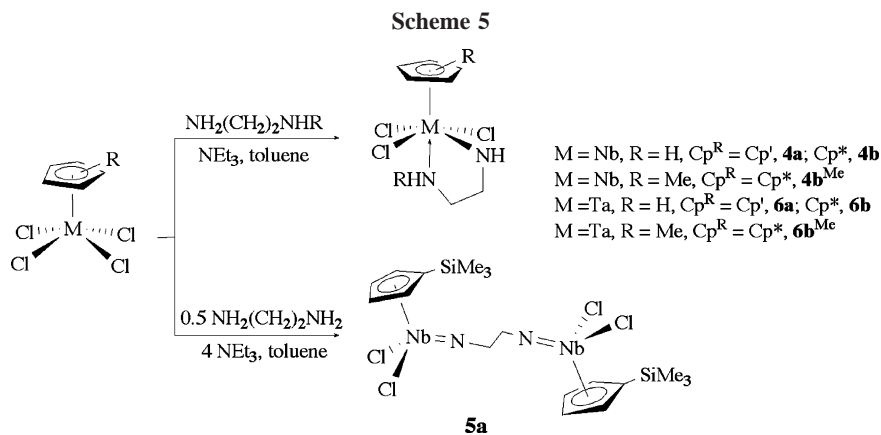
Reactions of Monocyclopentadienyl Niobium and Tantalum Derivatives with Diamines. The reactions described above were scaled-up, although the difficulty in isolating the different components of the reaction mixtures as analytically pure samples resulted in modest yields. Therefore, we sought a more convenient alternative synthetic route. In a procedure analogous to that used to synthesize the niobium⁴⁴ and titanium congeners,^{42,43} aminolysis reactions of [MCp^RCl₄] in aromatic solvents afforded the mononuclear amido-amino derivatives [MCp^R{NH(CH₂)₂-η-NHR}Cl₃] (M = Nb, R = H, Cp^R = Cp', **4a**; Cp*, **4b**; R = Me, Cp^R = Cp*, **4b**^{Me}; M = Ta, R = H, Cp^R = Cp', **6a**; Cp*, **6b**; R = Me, Cp^R = Cp*, **6b**^{Me}) and, in the particular case of niobium, the dinuclear complex [{NbCp^RCl₂}₂(μ-N(CH₂)₂-η-N)] (Cp^R = Cp', **5a**) by treatment of [MCp^RCl₄] with the appropriate amount of the corresponding ethylenediamine in toluene in the presence of NEt₃ (Scheme 5).

The different propensity of Nb–Cl and Ta–Cl bonds to undergo aminolysis was again made evident in these reactions. Thus, while the reaction of [NbCp^RCl₄] with 0.5 equiv of NH₂(CH₂)₂NH₂ in the presence of 4 equiv of NEt₃ yields the

(45) Ciruelos, S.; Cuenca, T.; Gómez, R.; Gómez-Sal, P.; Manzanero, A.; Royo, P. *Organometallics* **1996**, *15*, 5577–5585.

(46) Gómez, R.; Gómez-Sal, P.; Martín, A.; Nuñez, A.; del Real, P. A.; Royo, P. *J. Organomet. Chem.* **1998**, *564*, 93–100.

(47) Cuenca, T.; Royo, P. *Coord. Chem. Rev.* **1999**, *195*, 447–498.



tethered dinuclear imido complex **5a**, a similar reaction with the tantalum derivative never goes beyond the amido-amino compounds, even when an excess of triethylamine is used (the dinuclear imido derivative **5b** cannot be prepared through this reaction either). When the reaction of $[\text{TaCp}^*\text{Cl}_4]$ with 1 equiv of $\text{NH}_2(\text{CH}_2)_2\text{NHMe}$ was monitored by ^1H NMR (C_6D_6 or CDCl_3), formation of the intermediate adduct $[\text{TaCp}^*\text{Cl}_4\{\text{NH}_2(\text{CH}_2)_2\text{NHMe}\}]$ (**7**) was observed; this was slowly converted into the final amido-amino derivative **6b**^{Me}. [^1H NMR (400 MHz, C_6D_6) for $[\text{TaCp}^*\text{Cl}_4\{\text{NH}_2(\text{CH}_2)_2\text{NHMe}\}]$ (**7**): δ 0.03 (brs, 1H, *NHMe*), 1.92 (m, 2H, CH_2NHMe), 1.93 (s, 3H, *NHMe*), 2.35 (s, 15H, Cp^*), 3.36 (m, 2H, TaNHCH_2), 5.14 (brs, 2H, NH_2). $^{13}\text{C}\{^1\text{H}\}$ NMR (400 MHz, C_6D_6): δ 13.2 (C_5Me_5), 35.5 (CH_2NHMe), 44.1 (*NHMe*), 52.1 (TaNHCH_2), 132.4 (C_5Me_5).] In a preparative scale-up, reaction of $[\text{TaCp}^*\text{Cl}_4]$ with 2 equiv of $\text{NH}_2(\text{CH}_2)_2\text{NHMe}$ in aromatic solvents gave a mixture of the two isomers $[\text{TaCp}^*\{\text{NH}(\text{CH}_2)_2\text{-}\eta\text{-NHMe}\}\text{Cl}_3]$ (**6b**^{Me}) and $[\text{TaCp}^*\{\text{NMe}(\text{CH}_2)_2\text{-}\eta\text{-NH}_2\}\text{Cl}_3]$, which evolved into a pure sample of **6b**^{Me} when the mixture was dissolved in chlorinated solvents. [^1H NMR (400 MHz, C_6D_6) for $[\text{TaCp}^*\{\text{NMe}(\text{CH}_2)_2\text{-}\eta\text{-NH}_2\}\text{Cl}_3]$: δ 2.14 (s, 15H, Cp^*), 2.45 (m, 2H, CH_2NH_2), 3.13 (s, 3H, *TaNMe*), 3.53 (t, $J = 6$ Hz, 2H, *TaNMeCH}_2*), 4.26 (brs, 2, CH_2NH_2). $^{13}\text{C}\{^1\text{H}\}$ NMR (100.13 MHz, C_6D_6): δ 12.9 (C_5Me_5), 42.1 (CH_2NH_2), 52.9 (*TaNMe*), 67.7 (*TaNMeCH}_2*), 126.4 (C_5Me_5).] Treatment of $[\text{TaCp}^*\text{Cl}_4]$ with 0.5 equiv of ethylenediamine in the absence of NEt_3 afforded the dinuclear adduct $[\{\text{TaCp}^*\text{Cl}_4\}_2(\mu\text{-NH}_2(\text{CH}_2)_2\text{NH}_2)]$ (**8**) as a crystalline, orange solid, in high yield (Scheme 6). This complex was isolated and completely characterized by NMR spectroscopy and elemental analysis. In contrast, analogous niobium inter-

mediate adducts were not observed even when the reactions were carried out in the absence of NEt_3 . In this case, the ethylenediamine reagent itself acts as a base and the amido-amino derivatives **4** were straightforwardly formed, along with unreacted starting material.

Both types of niobium complexes (**4** and **5**) are formed quantitatively, although only compounds **4** were isolated as analytically pure solids. Instead, the extremely air- and moisture-sensitive compounds **5** precluded an accurate elemental analysis, with decomposition occurring in a matter of seconds. In fact, all attempts to crystallize **5a** were unsuccessful and gave mixtures of hydrolysis products, of which the main constituent is the tetranuclear niobium-oxo compound $[\{\text{NbCp}'\text{Cl}(\mu_2\text{-O})\}_4(\text{Cl})_2(\mu_3\text{-O})]$ (**9**), isolated by crystallization, and although it could not be characterized by NMR, as it was insoluble in all common deuterated solvents, its structure was unambiguously established by X-ray diffraction studies on a single crystal (see below). The tetranuclear nature of **9** is noteworthy since hydrolysis of monocyclopentadienyl complexes of niobium, under mild experimental conditions, usually renders dinuclear oxides.^{48–50} Such unusual behavior may be related to the dinuclear nature of compound **5a**.

The NMR spectroscopic features of these complexes support the proposed structure. C_s symmetry is established from the ^1H NMR spectra for compounds **4a**, **4b**, **6a**, and **6b** (see Experi-

(48) Andreu, A. M.; Jalón, F. A.; Otero, A.; Royo, P.; Lanfredi, A. M. M.; Tiripicchio, A. *J. Chem. Soc., Dalton Trans.* **1987**, 953–956.

(49) Bottomley, F.; Keizer, P. N.; White, P. S.; Preston, K. F. *Organometallics* **1990**, *9*, 1916–1925.

(50) Bottomley, F.; Karslioglu, S. *Organometallics* **1992**, *11*, 326–337.

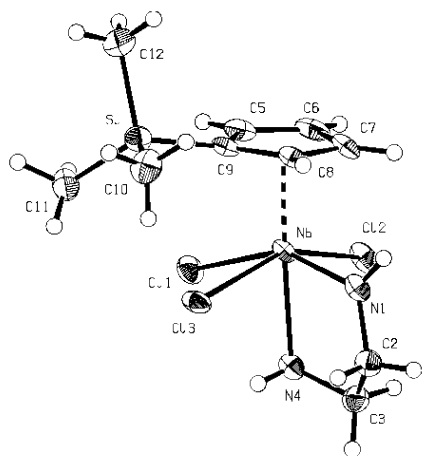


Figure 1. ORTEP-style representation of the molecular structure of complex **4a** as determined by single-crystal X-ray crystallography. Thermal ellipsoids are given at the 50% probability level.

mental Section). The spectra of **4b^{Me}** and **6b^{Me}** are consistent with chiral species demonstrated by the presence of two multiplets for the diastereotopic methylene protons in the corresponding ¹H NMR spectra and the expected resonances for the Cp* ring and methyl protons on silicon. This spectroscopic behavior undoubtedly indicates that the NHMe is fairly rigidly coordinated (the NHMe proton appearing as a broad signal and the NHMe hydrogens as a doublet) to the metal atom since such a bonding disposition prevents racemization at the amino nitrogen. The downfield shifted resonance observed for the amino functionality protons also supports such a bonding interaction. There was a notably higher chemical shift found for the amido proton (Nb $\delta \geq 9$ and Ta $\delta > 7$) with respect to other alkylamido derivatives of niobium and tantalum (normally in the region $\delta \approx 6$ –8 and $\delta \approx 5$).⁵¹ Such spectroscopic behavior can be attributed to the chelating disposition of the amido-amino ligand that forces the amido proton to approach the Cp^R ligand, locating this proton close enough to the cyclopentadienyl ring to experience the influence of its magnetic anisotropy. The structural characterization of **4a** confirms this observation (*vide infra*).

The spectroscopic behavior of **5** is relatively simple and supports a dinuclear species containing two spectroscopically equivalent C_s-symmetry metallic fragments. The ¹H NMR spectra show, along with the characteristic signals for the Cp^R ligand, a sharp singlet at δ 3.63 and 3.97 for **5a** and **5b**, respectively, and integration shows four protons assigned to the two magnetically equivalent methylene groups of the bridged chain. The high symmetry of compound **8** probably results in a ¹H NMR spectrum that displays only three signals, with integrals in the ratio 30:4:4 for the pentamethylcyclopentadienyl, methylene, and amino protons, respectively.

For all of these complexes, structural features similar to those described from ¹H NMR spectroscopy can be deduced from the ¹³C{¹H} NMR spectra, consistent with the proposed formulation and with the expected peaks observed in the region of the spectra typical of derivatives of this type.

Structural Studies. The molecular structures of compounds **4a** and **9** were determined by X-ray diffraction studies on a single crystal. The molecular structure of **4a** is shown in Figure 1, and key bond distances and angles are listed in Table 1. The crystal contains half of a molecule of benzene for each molecule

Table 1. Selected Bond Distances (Å) and Angles (deg) for Complexes **4a** and **9^a**

Compound 4a			
Nb–N(1)	1.992(4)	Cg–Nb–N(1)	102.5
Nb–N(4)	2.255(5)	Nb–N(1)–C(2)	122.9(3)
Nb–Cl(1)	2.511(1)	Nb–N(1)–H(11)	117(3)
Nb–Cl(2)	2.488(1)	C(2)–N(1)–H(11)	120(3)
Nb–Cl(3)	2.487(1)	C(3)–N(4)–Nb	112.9(3)
N(4)–H(41)···Cl(3)	2.57(5)	C(3)–N(4)–H(41)	115(3)
N(4)–H(42)···Cl(2)	2.72(6)	C(3)–N(4)–H(42)	111(4)
Compound 9			
Nb(1)–O(1)	1.885(3)	Nb(1)–O(1)–Nb(3)	110.68(16)
Nb(1)–O(3)	1.999(3)	Nb(3)–O(2)–Nb(2)	145.62(16)
Nb(1)–O(2)	2.164(3)	Nb(3)–O(2)–Nb(1)	98.94(13)
Nb(1)–Cl(11)	2.4363(13)	Nb(2)–O(2)–Nb(1)	95.16(13)
Nb(1)–Cl(12)	2.5806(12)	Nb(2)–O(3)–Nb(1)	107.09(15)
Nb(2)–O(3)	1.870(3)	Nb(4)–O(4)–Nb(2)	161.93(19)
Nb(2)–O(4)	2.023(3)	Nb(3)–O(5)–Nb(4)	155.05(19)
Nb(2)–O(2)	2.052(3)		
Nb(2)–Cl(2)	2.3976(14)		
Nb(3)–O(1)	1.992(3)		
Nb(3)–O(2)	2.032(3)		
Nb(3)–O(5)	1.843(3)		
Nb(3)–Cl(3)	2.4175(14)		
Nb(4)–O(4)	1.813(3)		
Nb(4)–O(5)	2.000(3)		
Nb(4)–Cl(41)	2.4246(16)		
Nb(4)–Cl(42)	2.4111(15)		

^a esd's are given in parentheses.

of **4a** in the lattice. The molecular structure shows **4a** to be a mononuclear species with a pseudo-octahedral coordination geometry around the niobium atom. The Cp' and the chelating ligand show *mer*-coordination, with the amino nitrogen virtually *trans* to the cyclopentadienyl group, a structural disposition that resembles that found for the constrained geometry complex [Nb{ η^5 -C₅H₄SiMe₂- η -N(CH₂)₃- η -NH₂}Cl₃].⁴⁴

The Cg–Nb–N1 (Cg = centroid of the Cp ring) bond angle of 102.5° is close to those found for the constrained geometry compounds [Nb{ η^5 -C₅H₄SiMe₂- η -N(CH₂)₃- η -NH₂}Cl₃]⁴⁴ (100.98°) and [Nb(η^5 -C₅H₄SiMe₂- η -NAr)(NAr)Cl]³² (100.76°) and is appreciably more acute than those reported in complexes bearing a normal monodentate amido group (106.60° to 116.67° range).^{27,31,34} The location of the amino nitrogen in the axial position (Cg–Nb–N4 \approx 176.3°), where coordination to the niobium atom seems to be optimal, and the chelating nature of the amido-amino ligand force the amido nitrogen out of the plane described by the three chlorine atoms, forward of the cyclopentadienyl ligand, according to the NMR spectroscopic observations. The amido and amino ligands have structurally different Nb–N–C linkages, distinguishable by differences in both the Nb–N bond lengths and the coordination environment at the nitrogen centers. As described above, the amido ligand is placed in the equatorial plane, allowing the filled p orbital on the N(1) to overlap with the unique π -acceptor orbital remaining on the niobium, located in this plane. The short Nb–N(1) bond distance (1.992(4) Å) is in the reported range for Nb–N bonds with an appreciable multiple-bond character (1.935–2.102 Å),⁵¹ and the planar environment of the N(1) atom, with the sum of the angles around it close to 360° and hence sp²-hybridized, suggests a perceptible N(p π)–Nb(d π) interaction. The coordination of the pendant NH₂ group is clearly shown with a Nb–N(4) distance of 2.255(5) Å, within the single-bond range (2.20–2.40 Å).^{52–55}

(52) Chesnut, R. W.; Fanwick, P. E.; Rothwell, I. P. *Inorg. Chem.* **1988**, *27*, 752–754.

(53) Jayaratne, K. C.; Yap, G. P. A.; Haggerty, B. S.; Rheingold, A. L.; Winter, C. H. *Inorg. Chem.* **1996**, *35*, 4910–4920.

(51) Humphries, M. J.; Green, M. L. H.; Leech, M. A.; Gibson, V. C.; Jolly, M.; Williams, D. N.; Elsegood, M. R. J.; Clegg, W. *J. Chem. Soc., Dalton Trans.* **2000**, 4044–4051.

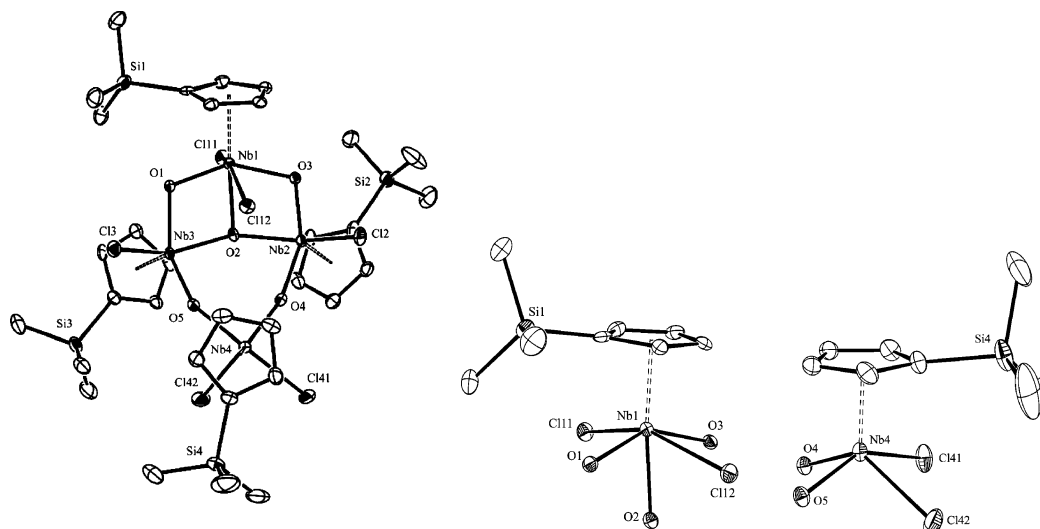


Figure 2. ORTEP view of **9** with 30% probability ellipsoids. Details of the coordination environment of Nb(1) and Nb(4) are shown.

Although all of the Nb–Cl distances are in the normal range for this type of bond, the Nb–Cl(1) bond *trans* to the amido group (2.511(1) Å) is somewhat elongated compared with the *cis* chloro bond (average 2.487(1) Å).

Of particular relevance are the two weak hydrogen bonds observed, which are nevertheless strong enough to introduce molecular recognition and self-assembly in the solid state.^{56,57} Thus, molecules of **4a** form infinite N–H⋯Cl hydrogen-bonded chains that propagate along the crystallographic *b*-axis. Each molecule donates two N–H⋯Cl hydrogen bonds and accepts two, which at 2.57(5) and 2.72(6) Å can be classified as “intermediate” (intermolecular contact in the range 2.52–2.95 Å).^{58,59}

Analysis of the X-ray data reveals **9** to be a tricyclic tetranuclear niobium oxide [$\{\text{NbCp}^{\text{R}}\text{Cl}(\mu_2\text{-O})\}_4(\text{Cl})_2(\mu_3\text{-O})$] that displays an unsymmetrical structure (Figure 2). The crystal contains half of a molecule of hexane (highly disordered) for each molecule of **9** in the lattice. This structure is particularly relevant because it is one of the scarce examples of clusters with more than three niobium or tantalum atoms.^{49,50,60–63} Selected bond distances and angles for the structure are listed in Table 1.

Complex **9** features a tricyclic structure defined by two Cp^RNbCl and two Cp^RNbCl₂ building units linked through four peripheral double oxo bridges and an intraannular triple oxo bridge. The core of cluster **9** resembles those found in several tetranuclear titanium oxides, [$\{\text{TiCp}^{\text{R}}(\mu_2\text{-O})\}_4\text{X}_2(\mu_2\text{-O})$],^{64,65} and has been described as a butterfly structure. However, in this case, the internal oxo bridge connects three of the niobium atoms ($\mu_3\text{-O}$), causing a notable distortion that becomes apparent in

the flattening of one of the butterfly wings. The core structure of **9** could be regarded as an “asymmetrical butterfly” where one of the wings is defined by a six-membered Nb₃O₃ ring, while the second one consists of two fused four-membered Nb₂O₂ rings sharing an NbO moiety.

The diverse coordination geometry shown by the two wing-tip niobium atoms undoubtedly reflects the presence of the triply connected oxygen site (see Figure 2). While Nb(4) is a five-coordinate center with a *cis* disposition, Nb(1) shows a pseudo-octahedral coordination geometry with both chlorine atoms mutually *trans* and the oxygen $\mu_3\text{-O}$ in an axial position. The closing of the Nb(1)–($\mu_2\text{-O}$)–Nb bond angles (Nb(1)–O(3)–Nb(2) [107.09(15)°] and Nb(1)–O(1)–Nb(3) [98.94(13)°]) and the contraction of the Nb(1)–Nb(adjacent) distances [3.1132(7) and 3.1902(7) Å] with respect to the corresponding values found around the Nb(4) atom (Nb(4)–O(4)–Nb(2) [161.93(19)°], Nb(4)–O(5)–Nb(3) [155.05(19)°], and Nb(4)–Nb(adjacent) [average 3.770 Å]) are unequivocally a consequence of the Nb(1)–O(2) bond presence. Both the Nb(1)–($\mu_2\text{-O}$)–Nb angles and the Nb(1)–Nb(adjacent) distances fall in the same ranges as those found in niobium triangular clusters.

The triply connected oxygen $\mu_3\text{-O}$ shows a significantly distorted pyramidal geometry, a rare structural feature, with two Nb–O–Nb angles remarkably more acute, Nb(1)–O(2)–Nb(3) [98.94(13)°] and Nb(1)–O(2)–Nb(2) [95.16(13)°], than the third, Nb(2)–O(2)–Nb(3) [145.62(16)°]. While the first two angles are within the values reported for a $\mu_3\text{-O}$ group in trinuclear niobium oxides, the latter is even more obtuse than that found for $\mu_2\text{-O}$ ligands in these very derivatives. This asymmetry is also manifested in the Nb–($\mu_3\text{-O}$) distances; thus, the $\mu_3\text{-O}$ ligand lies ca. 0.1 Å closer to the niobium atoms at the “butterfly hinge” [average 2.042 Å] than to the niobium atom at the tip of the wing; moreover the Nb(1)–O(2) distance [2.164(3) Å] is within the range observed for a dative covalent bond [2.16–2.39 Å range]. The double oxygen bridges in the core are markedly asymmetric; thus, for each Nb center, one of the Nb–O distances is between 0.12 and 0.20 Å longer than the other. These long and short distances are located in alternating positions along the perimeter core. The long length values are in the same range as those observed in trinuclear

(54) Corbin, R. A.; Dusick, B. E.; Phomphrai, K.; Fanwick, P. E.; Rothwell, I. P. *Chem. Commun.* **2005**, 1194–1196.

(55) Cotton, F. A.; Shang, M. Y. *J. Cluster Sci.* **1994**, *5*, 467–479.

(56) Desiraju, G. R. *Acc. Chem. Res.* **2002**, *35*, 565–573.

(57) Steiner, T. *Angew. Chem., Int. Ed.* **2002**, *41*, 48–76.

(58) Aullón, G.; Bellamy, D.; Brammer, L.; Bruton, E. A.; Orpen, A. G. *Chem. Commun.* **1998**, 653–654.

(59) Adams, N.; Bigmore, H. R.; Blundell, T. L.; Boyd, C. L.; Dubberley, S. R.; Sealey, A. J.; Cowley, A. R.; Skinner, M. E. G.; Mountford, P. *Inorg. Chem.* **2005**, *44*, 2882–2894.

(60) Gibson, V. C.; Kee, T. P.; Clegg, W. *J. Chem. Soc., Chem. Commun.* **1990**, 29–30.

(61) Jernakoff, P.; Debellefon, C. D.; Geoffroy, G. L.; Rheingold, A. L.; Geib, S. J. *Organometallics* **1987**, *6*, 1362–1364.

(62) De la Mata, J.; Fandos, R.; Gómez, M.; Gómez-Sal, P.; Martínez-Carrera, S.; Royo, P. *Organometallics* **1990**, *9*, 2846–2850.

(63) Leichtweis, I.; Roesky, H. W.; Noltemeyer, M.; Schmidt, H. G. *Chem. Ber.* **1991**, *124*, 253–257.

(64) Palacios, F.; Royo, P.; Serrano, R.; Balcazar, J. L.; Fonseca, I.; Florencio, F. *J. Organomet. Chem.* **1989**, *375*, 51–58.

(65) Babcock, L. M.; Klemperer, W. G. *Inorg. Chem.* **1989**, *28*, 2003–2007.

niobium complexes, while the small Nb–O distances are even shorter than those found in niobium dinuclear oxo derivatives, where a significant π -bonding contribution has been proposed.⁶⁶

The Nb–Cl lengths are reasonably similar. The one exception is the Nb(1)–Cl(12) distance of 2.5806(12) Å, which is considerably longer than the other Nb–Cl distances, averaging 2.417(1) Å. In addition, this chlorine deviates 0.557 Å from the Nb(1)O(2)Nb(4) plane that halves the core and is significantly closer to the Nb(2) center (2.950 Å) than to Nb(3) (3.440 Å). This asymmetry is also reflected in the Nb–Nb distances, with Nb(1) 0.08 Å closer to Nb(2) than to Nb(3).

In the molecular packing, the molecules are arranged in H-bonded chains along the crystallographic *b*-axis due to C–H \cdots Cl interactions between the chlorine atoms bonded to Nb(1) in a *trans* disposition to the Cp of adjacent molecules.

Conclusions

The formation of new types of tethered heterobimetallic titanium–niobium and titanium–tantalum complexes [TiCl₂{ η^5 -C₅H₄SiMe₂- η -N(CH₂)₂- κ -NH₂}MCP^RCl₄] (Cp^R = Cp', Cp*) has been described. These species evolve through different pathways from those described for the analogues complexes with a chlorosilyl-substituted cyclopentadienyl ring on the group 5 metal. In addition, a suitable and straightforward synthetic route to prepare and isolate mononuclear amido-amino complexes of niobium and tantalum, dinuclear imido derivatives of niobium, and amino compounds of tantalum in high yield is described. The structure of an unusual tricyclic tetranuclear niobium oxide [{NbCp^RCl(μ_2 -O)}₄(Cl)₂(μ_3 -O)], which displays a rare unsymmetrical triply connected oxygen site, is also reported.

Experimental Section

All manipulations were performed under an atmosphere of argon using standard Schlenk and glovebox techniques. The solvents were purified by distillation under argon before use by employing the appropriate drying/deoxygenated agent. Deuterated solvents were stored over activated 4 Å molecular sieves and degassed by several freeze–thaw cycles. NEt₃ (Aldrich) was distilled before use and stored over 4 Å molecular sieves. NH₂(CH₂)₂NH₂ (Aldrich) and NH₂(CH₂)₂NHMe (Aldrich) were purchased from commercial sources and used without further purification. [Ti{ η^5 -C₅H₄SiMe₂- η -N(CH₂)₂- η -NH₂}Cl₂]₄,⁴³ [NbCp^RCl₄],⁶⁷ [NbCp^RCl₄],^{62,68,69} [TaCp^RCl₄],⁶⁷ and [TaCp^RCl₄]^{70,71} were prepared as previously described. Elemental analyses were performed on a Perkin-Elmer 240B microanalyzer. Some of the analytical values found deviated (>1% C) due to their air sensitivity and difficulties in the manipulation of samples. NMR spectra were recorded on Varian Unity FT-300 and Bruker AV400 spectrometers, and chemical shifts are referenced to the residual proton and carbon signals of the solvent.

Synthesis of [TiCl₂{ η^5 -C₅H₄SiMe₂- η -N(CH₂)₂- κ -NH₂}Nb(η^5 -C₅H₄SiMe₃)Cl₄] (2a). A C₆D₆ solution (0.3 mL) of [Ti{ η^5 -C₅H₄SiMe₂-N(CH₂)₂- η -NH₂}Cl₂] (0.03 g, 0.1 mmol) was added to a C₆D₆ solution (0.3 mL) of [Nb(η^5 -C₅H₄SiMe₃)Cl₄] (0.037 g, 0.1 mmol)

(66) Skripkin, Y. V.; Eremenko, I. L.; Pasynskii, A. V.; Volkov, O. G.; Bakum, S. I.; Porai-Koshits, M. A.; Antsyshkina, A. S.; Dikareva, L. M.; Ostrikova, V. N.; Sahkarov, S. G.; Struchkov, Y. T. *Sov. J. Coord. Chem. (Engl. Transl.)* **1985**, *11*, 995–1002.

(67) Bunker, M. J.; Decian, A.; Green, M. L. H.; Moreau, J. J. E.; Sigantoria, N. *J. Chem. Soc., Dalton Trans.* **1980**, 2155–2161.

(68) Herrmann, W. A.; Kalcher, W.; Biersack, H.; Bernal, I.; Creswick, M. *Chem. Ber.* **1981**, *114*, 3558–3571.

(69) Yasuda, H.; Okamoto, T.; Nakamura, A. N. *Organomet. Synth.* **1988**, *4*, 20–22.

(70) Burt, R. J.; Chatt, J.; Leigh, G. J.; Teuben, J. H.; Westerhof, A. J. *Organomet. Chem.* **1977**, *129*, C33–C35.

(71) Sanner, R. D.; Carter, S. T.; Bruton, W. J. *J. Organomet. Chem.* **1982**, *240*, 157–162.

at room temperature. The color of the reaction mixture instantaneously darkened. The reaction mixture was analyzed by NMR spectroscopy, and the formation of **2a** was essentially quantitative. ¹H NMR (300 MHz, C₆D₆): δ 0.18 (s, 6H, SiMe₂N), 0.25 (s, 9H, SiMe₃), 3.54 (m, 2H, NCH₂CH₂NH₂), 4.10 (t, *J* = 5.8 Hz, 2H, NCH₂CH₂NH₂), 5.19 (brs, 2H, NH₂), 6.10, 6.35, 6.63, 6.84 (two AA'BB' spin system, 4 \times 2H, 2 \times C₅H₄). ¹³C{¹H} NMR (75 MHz, C₆D₆): δ -2.6 (SiMe₂N), -0.1 (SiMe₃), 47.5 (CH₂NH₂), 58.0 (TiNCH₂), 109.3 (C₅H₄SiN-*Cipso*), 124.3, 126.4, 132.0, 132.4, 135.1 (C₅H₄).

Synthesis of [TiCl₂{ η^5 -C₅H₄SiMe₂- η -N(CH₂)₂- κ -NH₂}Nb(η^5 -C₅Me₃)Cl₄] (2b). A method similar to that used for **2a** was adopted by using [Nb(η^5 -C₅Me₃)Cl₄] (0.037 g, 0.1 mmol) to give **2b**. ¹H NMR (300 MHz, C₆D₆): δ 0.20 (s, 6H, SiMe₂N), 2.05 (s, 15H, Cp*), 3.55 (m, 2H, NCH₂CH₂NH₂), 4.11 (t, *J* = 5.7 Hz, 2H, NCH₂-CH₂NH₂), 4.96 (brs, 2H, NH₂), 6.11, 6.35 (AA'BB' spin system, 2 \times 2H, C₅H₄).

Synthesis of [TiCl₂{ η^5 -C₅H₄SiMe₂- η -N(CH₂)₂- κ -NH₂}Ta(η^5 -C₅H₄SiMe₃)Cl₄] (3a). A CDCl₃ solution (0.3 mL) of [Ti{ η^5 -C₅H₄-SiMe₂-N(CH₂)₂- η -NH₂}Cl₂] (0.03 g, 0.1 mmol) was added to a CDCl₃ solution (0.3 mL) of [Ta(η^5 -C₅H₄SiMe₃)Cl₄] (0.046 g, 0.1 mmol) at room temperature. The reaction mixture was analyzed by NMR spectroscopy, and the formation of **3a** was essentially quantitative. ¹H NMR (300 MHz, CDCl₃): δ 0.36 (s, 9H, SiMe₃), 0.57 (s, 6H, SiMe₂), 3.59 (m, 2H, NCH₂CH₂NH₂), 4.56 (t, *J* = 5.7 Hz, 2H, NCH₂CH₂NH₂), 4.83 (brs, 2H, NH₂), 6.57, 6.79 (AA'BB' spin system, 2 \times 2H, C₅H₄), 7.03 (m, 4H, C₅H₄).

Synthesis of [TiCl₂{ η^5 -C₅H₄SiMe₂- η -N(CH₂)₂- κ -NH₂}Ta(η^5 -C₅Me₃)Cl₄] (3b). A method similar to that used for **3a** was adopted by using [Ta(η^5 -C₅Me₃)Cl₄] (0.046 g, 0.1 mmol) to give **3b**. ¹H NMR (300 MHz, CDCl₃): δ 0.58 (s, 6H, SiMe₂N), 2.56 (s, 15H, Cp*), 3.54 (m, 2H, NCH₂CH₂NH₂), 4.56 (t, *J* = 6.0 Hz, 2H, NCH₂-CH₂NH₂), 4.61 (brs, 2H, NH₂), 6.57, 7.01 (AA'BB' spin system, 2 \times 2H, C₅H₄). ¹³C{¹H} NMR (75 MHz, CDCl₃): δ -2.1 (SiMe₂N), 13.2 (C₅Me₃), 46.5 (CH₂NH₂), 58.8 (TiNCH₂), 109.4 (C₅H₄SiN-*Cipso*), 124.3, 126.7 (C₅H₄), 132.9 (C₅Me₃).

Synthesis of [Nb(η^5 -C₅H₄SiMe₃)(NH(CH₂)₂- η -NH₂)Cl₃] (4a). **Method a.** A toluene solution (20 mL) of [Ti{ η^5 -C₅H₄SiMe₂- η -N(CH₂)₂-NH₂}Cl₂] (0.50 g, 1.67 mmol) was added to a toluene solution (30 mL) of [Nb(η^5 -C₅H₄SiMe₃)Cl₄] (0.62 g, 1.67 mmol) at room temperature. The reaction mixture was stirred for 4 h and concentrated under vacuum to ca. half volume. After standing at room temperature for 24 h, pale green crystals of **4a** precipitated from the solution, which were collected and dried under vacuum (0.31 g, 0.78 mmol, yield 47%).

Method b. A toluene solution (20 mL) of NH₂(CH₂)₂NH₂ (0.09 mL, 1.34 mmol) and NEt₃ (0.20 mL, 1.40 mmol) was added to dark green solution of [Nb(η^5 -C₅H₄SiMe₃)Cl₄] (0.5 g, 1.34 mmol) in toluene (30 mL). The color of the reaction mixture immediately changed to dark green. The reaction mixture was stirred for 3 h and the white solid formed collected by filtration. The solution was concentrated (20 mL) and cooled to -20 °C. After filtration, recrystallization from toluene/hexane gave **4a** in 96% yield (0.51 g, 1.29 mmol). Anal. Calcd for C₁₀H₂₀Cl₃N₂NbSi: C, 30.35; H, 5.10; N, 7.07. Found: C, 30.61; H, 5.20; N, 6.97. ¹H NMR (300 MHz, CDCl₃): δ 0.38 (s, 9H, SiMe₃), 3.63 (m, 2H, CH₂NH₂), 4.10 (m, 2H, NbNHCH₂), 5.12 (brs, 2H, NH₂), 6.66, 6.95 (AA'BB' spin system, 2 \times 2H, C₅H₄), 10.23 (brs, 1H, NbNHCH₂). ¹³C{¹H} NMR (75 MHz, CDCl₃): δ 0.15 (SiMe₃), 43.9 (CH₂NH₂), 61.7 (NbN-HCH₂), 123.7, 123.9 (C₅H₄), 128.7 (C₅H₄-*ipso*).

Synthesis of [Nb(η^5 -C₅Me₃)(NH(CH₂)₂- η -NH₂)Cl₃] (4b). **Method a.** A method similar to method a described for **4a** was adopted by using [Nb(η^5 -C₅Me₃)Cl₄] (0.30 g, 0.81 mmol). Compound **4b** was obtained as an orange, microcrystalline solid in 31.3% yield (0.1 g, 0.25 mmol).

Method b. A method similar to method b described for **4a** was adopted by using [Nb(η^5 -C₅Me₃)Cl₄] (0.30 g, 0.81 mmol) to give

4b. Yield: 86.3% (0.1 g, 0.25 mmol). Anal. Calcd for $C_{12}H_{22}Cl_3N_2-Nb$: C, 36.62; H, 5.64; N, 7.11. Found: C, 37.03; H, 5.77; N, 6.76. 1H NMR (300 MHz, $CDCl_3$): δ 2.22 (s, 15H, Cp*), 3.35 (m, 2H, CH_2NH_2), 4.07 (m, 2H, NbNHCH₂), 5.07 (brs, 2H, NH₂), 8.96 (brs, 1H, NbNHCH₂). $^{13}C\{^1H\}$ NMR (75 MHz, $CDCl_3$): δ 13.0 (C_5Me_5), 43.6 (CH_2NH_2), 60.8 (NbNCH₂), 127.6 (C_5Me_5).

Synthesis of $[Nb(\eta^5-C_5Me_5)(NH(CH_2)_2-\eta-NHMe)Cl_3]$ (4b^{Me}**).** A method similar to method b described for **4a** was adopted by using $NH_2(CH_2)_2NHMe$ (0.05 mL, 0.57 mmol) and $[Nb(\eta^5-C_5Me_5)Cl_4]$ (0.21 g, 0.57 mmol) to give **4b^{Me}**. Total yield: 78.8% (0.18 g, 0.45 mmol). Anal. Calcd for $C_{13}H_{24}Cl_3N_2Nb$: C, 38.30; H, 5.95; N, 6.87. Found: C, 38.17; 6.35 H; 6.34 N. 1H NMR (300 MHz, $CDCl_3$): δ 2.12 (s, 15H, C_5Me_5), 3.06 (d, $J = 5.6$ Hz, 3H, NHMe), 3.21, 3.34 (m, 2 \times 1H, CH_2NHMe), 3.90 (m, 2H, NbNHCH₂), 5.30 (brs, 1H, NHMe), 8.99 (brs, 1H, NbNHCH₂). $^{13}C\{^1H\}$ NMR (75 MHz, $CDCl_3$): δ 13.2 (C_5Me_5), 40.7 (CH_2NHMe), 53.9 (NHMe), 57.0 (NbNCH₂), 127.5 (C_5Me_5).

Synthesis of $[Ta(\eta^5-C_5H_4SiMe_3)(NH(CH_2)_2-\eta-NH_2)Cl_3]$ (6a**).** **Method a.** A dichloromethane solution (20 mL) of $[Ti\{\eta^5-C_5H_4SiMe_2-\eta-N(CH_2)_2NH_2\}Cl_2]$ (0.39 g, 1.30 mmol) was added to a dichloromethane solution (50 mL) of $[Ta(\eta^5-C_5H_4SiMe_3)Cl_4]$ (0.60 g, 1.30 mmol) at room temperature. After stirring was continued for a week, the volatiles were removed under vacuum and the resulting solid washed with toluene (5 \times 10 mL). The yellow residue was identified as **6a** (0.22 g, 0.46 mmol, 35% yield).

Method b. A toluene solution (20 mL) of $NH_2(CH_2)_2NH_2$ (0.066 mL, 0.98 mmol) and NEt_3 (0.14 mL, 1.0 mmol) was added to a dark green solution of $[Ta(\eta^5-C_5H_4SiMe_3)Cl_4]$ (0.45 g, 0.98 mmol) in toluene (60 mL). After stirring for 3 h, the solution was filtered and volatiles were completely removed. The residue was extracted into toluene (2 \times 20 mL), and the solution obtained was concentrated (30 mL) and cooled to -20 °C. After filtration, recrystallization from toluene/hexane gave **6a** in 82% yield (0.39 g, 0.80 mmol). Anal. Calcd for $C_{10}H_{20}Cl_3N_2SiTa$: C, 24.83; H, 4.17; N, 5.79. Found: C, 24.97; H, 4.35; N, 6.16. 1H NMR (300 MHz, $CDCl_3$): δ 0.35 (s, 6H, $SiMe_3$), 3.60 (m, 2H, CH_2NH_2), 4.33 (m, 2H, TaNHCH₂), 4.87 (brs, 2H, NH₂), 6.43, 6.75 (AA'BB' spin system, 2 \times 2H, C_5H_4), 8.45 (brs, 1H, TaNHCH₂). $^{13}C\{^1H\}$ NMR (75 MHz, $CDCl_3$): δ 0.12 ($SiMe_3$), 43.7 (CH_2NH_2), 7.3 (TaNHCH₂), 121.3, 121.4 (C_5H_4), 125.6 (C_5H_4 -*ipso*).

Synthesis of $[Ta(\eta^5-C_5Me_5)(NH(CH_2)_2-\eta-NH_2)Cl_3]$ (6b**).** **Method a.** A dichloromethane solution (20 mL) of $[Ti\{\eta^5-C_5H_4SiMe_2-\eta-N(CH_2)_2NH_2\}Cl_2]$ (0.26 g, 0.87 mmol) was added to a dichloromethane solution (50 mL) of $[Ta(\eta^5-C_5Me_5)Cl_4]$ (0.40 g, 0.87 mmol). The solution was stirred for 2 weeks at 60 °C, when volatiles were completely removed. The residue was washed with *n*-hexane (5 \times 20 mL) and extracted into toluene (2 \times 50 mL). The resulting solution was concentrated and cooled to -20 °C to afford **6a** in 51% yield (0.21 g, 0.44 mmol).

Method b. A method similar to method b described for **6a** was adopted by using $[Ta(\eta^5-C_5Me_5)Cl_4]$ (0.24 g, 0.66 mmol) to give **6b**. Yield: 76% (0.1 g, 0.50 mmol). Anal. Calcd for $C_{12}H_{22}Cl_3N_2-Ta$: C, 29.92; H, 4.61; N, 5.81. Found: C, 30.05; H, 4.98; N, 5.64. 1H NMR (300 MHz, $CDCl_3$): δ 2.29 (s, 15H, Cp*), 3.54 (m, 2H, CH_2NH_2), 4.24 (m, 2H, TaNHCH₂), 4.84 (brs, 2H, NH₂), 7.35 (brs, 1H, TaNHCH₂). $^{13}C\{^1H\}$ NMR (75 MHz, $CDCl_3$): δ 12.4 (C_5Me_5), 43.6 (CH_2NH_2), 59.9 (NbNCH₂), 124.2 (C_5Me_5).

Synthesis of $[Ta(\eta^5-C_5Me_5)(NH(CH_2)_2-\eta-NHMe)Cl_3]$ (6b^{Me}**).** A method similar to method b described for **6a** was adopted by using $NH_2(CH_2)_2NHMe$ (0.058 mL, 0.65 mmol) and $[Ta(\eta^5-C_5Me_5)Cl_4]$ (0.30 g, 0.65 mmol) to give **6b^{Me}**. Yield: 76% (0.24 g, 0.50 mmol). Anal. Calcd for $C_{13}H_{24}Cl_3N_2Ta$: C, 31.50; H, 4.89; N, 5.65. Found: C, 31.40; H, 4.61; N, 5.39. 1H NMR (300 MHz, $CDCl_3$): δ 2.29 (s, 15H, Cp*), 3.17 (d, $J = 6$ Hz, 3H, NHMe), 3.25, 3.46 (m, 2 \times 1H, CH_2NHMe), 4.07, 4.16 (m, 2 \times 1H, TaNHCH₂), 5.02 (brs, 1H, NHMe), 7.40 (brs, 1H, TaNHCH₂). ^{13}C

$\{^1H\}$ NMR (75 MHz, $CDCl_3$): δ 12.6 (C_5Me_5), 40.5 (NHMe), 53.2 (TaNHCH₂), 54.9 (CH_2NHMe), 124.2 (C_5Me_5).

Synthesis of of $[Nb(\eta^5-C_5H_4SiMe_3)Cl_2](\mu-N(CH_2)_2-\eta-N)]$ (5a**).** A toluene solution (10 mL) of $NH_2(CH_2)_2NH_2$ (0.045 mL, 0.67 mmol) and NEt_3 (0.75 mL, 5.36 mmol) was added to a solution of $[Nb(\eta^5-C_5H_4SiMe_3)Cl_4]$ (0.50 g, 1.34 mmol) in toluene (20 mL). After overnight stirring, the initial dark green color changed to orange-brown and a white solid precipitated. The suspension was filtered, volatiles were removed, and the brown residue was extracted into *n*-hexane (5 \times 20 mL). The yellow filtrate was concentrated to ca. 60 mL and cooled to -20 °C. After filtration, recrystallization from toluene/hexane gave **5a** as a yellow solid in 58% yield (0.25 g, 0.39 mmol). Anal. Calcd for $C_{18}H_{30}Cl_4N_2Nb_2-Si_2$: C, 32.84; H, 4.60; N, 4.25. Found: C, 31.20; H, 4.24; N, 3.01. The isolated pale orange solid consisted mainly of **5a**, but it contained some irremovable decomposition products, which prevented us from obtaining a correct elemental analysis, though satisfactory spectroscopy data were obtained. 1H NMR (300 MHz, C_6D_6): δ 0.22 (s, 18H, $SiMe_3$), 3.63 (s, 4H, CH_2), 6.23, 6.39 (AA'BB' spin system, 2 \times 4H, C_5H_4). $^{13}C\{^1H\}$ NMR (75 MHz, C_6D_6): δ -0.56 ($SiMe_2$), 67.1 (CH_2), 113.7, 122.7 (C_5H_4), 134.6 (C_5H_4 -*ipso*).

Synthesis of $[Nb(\eta^5-C_5Me_5)Cl_2](\mu-N(CH_2)_2-\eta-N)]$ (5b**).** A toluene solution (20 mL) of $[Ti\{\eta^5-C_5H_4SiMe_2-\eta-N(CH_2)_2NH_2\}Cl_2]$ (0.24 g, 0.80 mmol) was added to a toluene solution (30 mL) of $[Nb(\eta^5-C_5Me_5)Cl_4]$ (0.30 g, 0.81 mmol) at room temperature. The reaction mixture was stirred for 4 h and cooled to -20 °C. After removing the precipitated solid (**4b**), the resulting yellow solution was taken to dryness and the solid residue was recrystallized from toluene/hexane to give **5b** as a pale orange solid in 5% yield (0.013 g, 0.02 mmol). Anal. Calcd for $C_{22}H_{34}Cl_4N_2Nb_2$: C, 40.39; H, 5.25; N, 4.28. Found: C, 37.96; H, 4.20; N, 3.12. The isolated pale orange solid consisted mainly of **5b**, but it contained some irremovable decomposition products, which prevented us from obtaining correct elemental analysis, though satisfactory spectroscopy data were obtained. 1H NMR (300 MHz, C_6D_6): δ 1.78 (s, 30H, Cp*), 3.97 (s, 4H, CH_2).

Synthesis of $[TaCp^*Cl_4](\mu-NH_2(CH_2)_2NH_2)]$ (8**).** A toluene solution (20 mL) of $NH_2(CH_2)_2NH_2$ (0.03 mL, 0.44 mmol) was added to a yellow solution of $[Ta(\eta^5-C_5Me_5)Cl_4]$ (0.40 g, 0.88 mmol) in toluene (50 mL). After being stirred for 1 h, the resulting solution was concentrated (30 mL) and cooled to -20 °C. After filtration, recrystallization from toluene/hexane gave **8** as an orange microcrystalline solid in 84.1% yield (0.36 g, 0.37 mmol). Anal. Calcd for $C_{22}H_{38}Cl_8N_2Ta_2$: C, 27.07; H, 3.93; N, 2.87. Found: C, 26.62; H, 4.19; N, 2.97. 1H NMR (300 MHz, $CDCl_3$): δ 2.58 (s, 30H, Cp*), 3.67 (m, 4H, CH_2), 4.50 (m, 4H, NH₂). $^{13}C\{^1H\}$ NMR (75 MHz, $CDCl_3$): δ 13.4 (C_5Me_5), 46.5 (CH_2), 133.0 (C_5Me_5).

Synthesis of $\{Nb(\eta^5-C_5H_4SiMe_3)(Cl)(\mu_2-O)\}_4(Cl)_2(\mu_3-O)$ (9**).** When a pentane or hexane solution of **5a** was allowed to stand in dry ice for several weeks, a crop of pale yellow crystals of **9** was formed. Anal. Calcd for $C_{32}H_{52}Cl_6Nb_4O_5Si_4$: C, 31.67; H, 4.33. Found: C, 31.63; H, 4.50. The isolated pale yellow solid consisted of **9** according to the elemental analysis data and the X-ray diffraction studies, but it was insoluble in all deuterated solvents, which prevented us from obtaining satisfactory spectroscopy data.

Single-Crystal X-ray Structure Determination of Compounds **4a·0.5(C_6H_6) and **9**·0.5(C_6H_{14}).** Crystal data and details of the structure determination are presented in Table 2. Suitable single crystals of **4a** for the X-ray diffraction study were grown from benzene. A clear, colorless needle was stored under perfluorinated ether, transferred in a Lindemann capillary, fixed, and sealed. Preliminary examination and data collection were carried out on an area detecting system (NONIUS, MACH3, κ -CCD) at the window of a rotating anode (NONIUS, FR591) with graphite-monochromated Mo $K\alpha$ radiation ($\lambda = 0.71073$ Å). The unit cell parameters were obtained by full-matrix least-squares refinement

Table 2. Crystallographic Data for **4a** and **9**

	4a ·0.5(C ₆ H ₆)	9 ·0.5(C ₆ H ₁₄)
formula	C ₁₃ H ₂₃ Cl ₃ N ₂ NbSi	C ₃₅ H ₅₉ O ₅ Cl ₆ Si ₄ Nb ₄
fw	434.68	1256.52
color/habit	colorless/needle	yellow/prism
cryst dimens, mm ³	0.10 × 0.13 × 0.41	0.25 × 0.20 × 0.03
cryst syst	monoclinic	triclinic
space group	P2 ₁ /c (no. 14)	P1 (no. 2)
a, Å	15.0441(5)	7.6685(7)
b, Å	8.9527(4)	14.7194(16)
c, Å	14.3759(6)	23.0373(19)
α, deg	90	80.411(7)
β, deg	109.386(2)	82.007(7)
γ, deg	90	81.343(7)
V, Å ³	1862.45(13)	2517.4(4)
Z	4	2
T, K	123	200
D _{calcd} , g cm ⁻³	1.581	1.658
μ, mm ⁻¹	1.156	1.337
F(000)	884	1262
θ range, deg	2.69–25.31	3.58–27.50
index ranges (h, k, l)	±18, ±10, ±17	±9, ±19, ±29
no. of reflns collected	9138	20 936
no. of indep reflns/R _{int}	3314/0.033	11 283/0.0810
no. of obsd reflns (I > 2σ(I))	2990	6841
no. of data/restraints/ params	3314/0/273	11 283/0/484
R1/wR2 (I > 2σ(I)) ^a	0.0388/0.0958	0.0559/0.0802
R1/wR2 (all data) ^a	0.0449/0.0982	0.1218/0.0933
GOF (on F ²) ^a	1.236	0.986
largest diff peak and hole, e Å ⁻³	+0.84/−0.45	+0.802/−0.712

^a R1 = $\sum(|F_o| - |F_c|)/\sum|F_o|$; wR2 = $\{\sum[w(F_o^2 - F_c^2)^2]/\sum[w(F_o^2)^2]\}^{1/2}$; GOF = $\{\sum[w(F_o^2 - F_c^2)^2]/(n - p)\}^{1/2}$.

of 25 339 reflections. Data collection was performed at 123 K (Oxford Cryosystems) within a θ range of $2.69^\circ < \theta < 25.31^\circ$. Four data sets were measured in rotation scan modus with $\Delta\varphi/\Delta\omega = 1.0^\circ$. A total number of 9138 intensities were integrated. Raw data were corrected for Lorentz, polarization, and, arising from the scaling procedure, latent decay and absorption effects. After merging ($R_{\text{int}} = 0.033$), a sum of 3314 (all data) and 2990 [$I > 2\sigma(I)$], respectively, remained and all data were used. The structures were solved by a combination of direct methods and difference Fourier syntheses. All non-hydrogen atoms were refined with anisotropic displacement parameters. All hydrogen atoms could be located in the final difference Fourier maps and were allowed to refine with individual isotropic displacement parameters. Full-matrix least-squares refinements with 273 parameters were carried out by minimizing $\sum w(F_o^2 - F_c^2)^2$ with the SHELXL-97 weighting scheme and stopped at shift/err < 0.001. The final residual electron density maps showed no remarkable features. Neutral atom scattering factors for all atoms and anomalous dispersion corrections for the non-hydrogen atoms were taken from *International Tables for Crystallography*. All calculations were performed on an Intel

Pentium 4 PC, with the STRUX-V system, including the programs PLATON, SIR92, and SHELXL-97.^{72–77}

Suitable single crystals of **9** for the X-ray diffraction study were grown from hexane. A yellow crystal was selected, covered with perfluorinated ether, and mounted on a Bruker-Nonius Kappa CCD single-crystal diffractometer equipped with graphite-monochromated Mo K α radiation ($\lambda = 0.71073$ Å). Data collection was performed at 200(2) K. Multiscan⁷⁸ absorption correction procedures were applied to the data. The structures were solved, using the WINGX package,⁷⁹ by direct methods (SHELXS-97) and refined by using full-matrix least-squares against F^2 (SHELXL-97).^{72–77} All non-hydrogen atoms were anisotropically refined, except for the carbon atoms in a very disordered hexane molecule. Hydrogen atoms were geometrically placed and left riding on their parent atoms except for the hydrogens in the disorder solvent molecule that could not be placed. Full-matrix least-squares refinements with 484 parameters were carried out by minimizing $\sum w(F_o^2 - F_c^2)^2$ with the SHELXL-97 weighting scheme and stopped at shift/err < 0.001. The final residual electron density maps showed no remarkable features.

Crystallographic data (excluding structure factors) for the structures reported in this paper have been deposited with the Cambridge Crystallographic Data Centre as supplementary publication nos. CCDC-641147 [**4a**·0.5(C₆H₆)] and CCDC-636015 [**9**·0.5(C₆H₁₄)]. Copies of the data can be obtained free of charge on application to CCDC, 12 Union Road, Cambridge CB2 1EZ, UK (fax: (+44)1223-336-033; e-mail: deposit@ccdc.cam.ac.uk).

Acknowledgment. Financial support for this research by DGICYT (Project MAT2004-02614) and CAM (Project GR/MAT/0622/2004) is gratefully acknowledged. M.C.M. and C.P. acknowledge Universidad de Alcalá for fellowships.

Supporting Information Available: Tables of crystallographic data, including fractional coordinates, bond lengths and angles, anisotropic displacement parameters, and hydrogen atom coordinates of complexes **4a**·0.5(C₆H₆) and **9**·0.5(C₆H₁₄). NMR spectra of complexes **2a**, **2b**, **3a**, **3b**, **5a**, and **5b**. This material is available free of charge via the Internet at <http://pubs.acs.org>.

OM7002927

(72) *Data Collection Software for Nonius k-CCD devices*; Delft, The Netherlands, 1999.

(73) Otwinowski, Z.; Minor, W. *Methods Enzymol.* **1997**, *276*, 307–326.

(74) Altomare, A.; Cascarano, G.; Giacovazzo, C.; Guagliardi, A.; Burla, M. C.; Polidori, G.; Camalli, M. *SIR92. J. Appl. Crystallogr.* **1994**, *27*, 435–436.

(75) *International Tables for Crystallography*; Wilson, A. J. C., Ed.; Kluwer Academic Publishers: Dordrecht, The Netherlands, 1992; Vol. C, Tables 6.1.1.4, 4.2.6.8, and 4.2.4.2.

(76) Spek, A. L. *PLATON*, A Multipurpose Crystallographic Tool; Utrecht University: Utrecht, The Netherlands, 2001.

(77) Sheldrick, G. M. *SHELXL-97*; Universität Göttingen: Göttingen, Germany, 1998.

(78) Blessing, R. H. *SORTA V. Acta Crystallogr. Sect. A* **1995**, *51*, 33–38.

(79) Farrugia, L. J. *J. Appl. Crystallogr.* **1999**, *32*, 837–938.